

Gas Hydrate Single-Crystal Structure Analyses

Michael T. Kirchner,[†] Roland Boese,^{*,†} W. Edward Billups,[‡] and Lewis R. Norman[§]

Contribution from the Institut für Anorganische Chemie der Universität Duisburg-Essen, Campus Essen, 45117 Essen, Germany, the Department of Chemistry, Rice University, Houston, Texas 77251, and Halliburton Company, Technology Center, 2600 S. 2nd Street, Duncan, Oklahoma 73536-0470

Received February 11, 2004; E-mail: roland.boese@uni-essen.de

Abstract: The first single-crystal diffraction studies on methane, propane, methane/propane, and adamantane gas hydrates SI, SII, and SH have been performed. To circumvent the problem of very slow crystal growth, a novel technique of in situ cocrystallization of gases and liquids resulting in oligocrystalline material in a capillary has been developed. With special data treatment, termed oligo diffractometry, structural data of the gas hydrates of methane, acetylene, propane, a propane/ethanol/methane-mixture and an adamantane/methane-mixture were obtained. Cell parameters are in accord with reported values. Host network and guest are subject to extensive disorder, reducing the reliability of structural information. It was found that most cages are fully occupied by a guest molecule with the exception of the dodecahedral cage in the acetylene hydrate which is only filled to 60%. For adamantane in the icosahedral cage a disordered model is proposed.

Introduction

Although gas hydrates were discovered in 1811 by Sir H. Davy,¹ they were regarded as a laboratory curiosity until the mid 1930s. After clathrate hydrates of natural gases were identified as the reason for plugging of gas pipelines, extensive efforts aimed at ways to reduce the substantial costs of keeping pipelines free of gas hydrates were initiated. Interest in gas hydrates further increased when deep sea exploration identified huge reservoirs of methane gas in hydrate form, probably exceeding other fossil fuel reserves by a factor of 2.¹ Structural details appeared in 1951 when Claussen proposed a structure based on ab initio calculations that was soon proven to be correct by von Stackelberg.²

Three main structural types of gas hydrates, named SI, SII, and SH, have been characterized in their single crystals using neutron or X-ray diffraction techniques.^{3,4,5} Recently, other types have been reported.⁶

Within the family of inclusion compounds, gas hydrates represent an extraordinary category. The host network consists of cages which are built from water molecules that incorporate

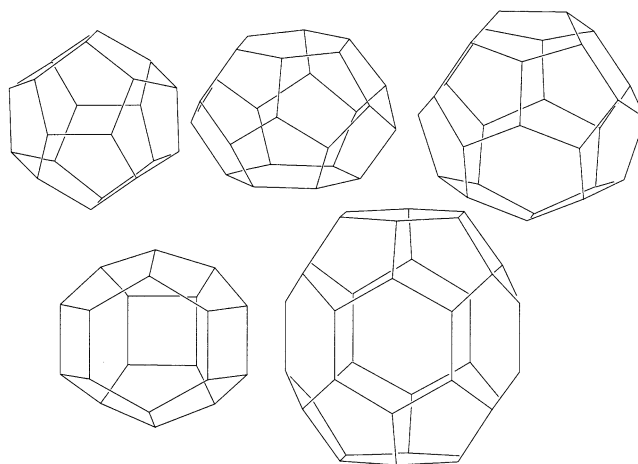


Figure 1. Cage shapes in the clathrates. From left to right, top row: dodecahedron, tetrakaidecahedron, hexakaidecahedron; bottom row: irregular dodecahedron and icosahedron.

guest molecules. The most important networks are structure I, $6X \cdot 2Y \cdot 46H_2O$, structure II, $8X \cdot 16Y \cdot 136H_2O$, and the hexagonal structure H, $1X \cdot 3Y \cdot 2Z \cdot 34H_2O$, where X, Y, and Z indicate different types of cages in the clathrate hydrates, according to their size. The cages are filled with guest molecules that stabilize the host network. An overview of the prominent cages and the nomenclature are presented in Figure 1.

Diffraction experiments have been performed on single crystals from mixtures of ethylene oxide, tetrachloromethane, and dimethylpentane with water.^{3,4,5} Xenon and hydrogen sulfide were used as *help gases* with tetrachloromethane and dimethylpentane. Crystallization times of several months up to six years have been reported. It should be noted that these crystallization experiments have been performed with liquid guests that are

[†] University of Duisburg-Essen.

[‡] Rice University, Houston.

[§] Halliburton Company, Duncan.

- (1) Sloan, E. D. *Clathrate Hydrates of Natural Gases*; Dekker: New York, 1998.
- (2) Claussen, W. F. *J. Chem. Phys.* **1951**, *19*, 662; von Stackelberg, M.; Müller, H. R. *Naturwiss.* **1951**, *38*, 456.
- (3) McMullan, R. K.; Jeffrey, G. A. *J. Chem. Phys.* **1965**, *42*, 2725.
- (4) Mak, T. C. W.; McMullan, R. K. *J. Chem. Phys.* **1965**, *42*, 2732; Hollander, F.; Jeffrey, G. A. *J. Chem. Phys.* **1977**, *66*, 4699–4705; McMullan, R. K.; Kvik, Å. *Acta Crystallogr.* **1990**, *B46*, 390–399.
- (5) Udachin, K. A.; Ratcliffe, C. I.; Enright, G. D.; Ripmeester, J. A. *Supramol. Chem.* **1997**, *8*, 173–176.
- (6) Udachin, K. A.; Ripmeester, J. A. *Nature (London)* **1999**, *397*, 420–423; Udachin, K. A.; Ratcliffe, C. I.; Ripmeester, J. A. *Angew. Chem., Int. Ed. Engl.* **2001**, *40*, 1303.

easier to handle. The difficulty in obtaining single crystals of good quality by cocrystallization of a gas and a liquid is due to the diffusion barrier of the solid product between the gas and the liquid phase. Consequently, the clathrate hydrates of natural gases have been investigated primarily by neutron powder diffraction.⁷ As compared to single-crystal structure determination, powder diffraction techniques leave a residual uncertainty because of the required assumptions due to the low data/parameter ratio.

We report here the crystallization and X-ray analysis of clathrate hydrates of SI from methane **1** and acetylene **2**, SII from propane **3** and a mixture **4** of propane and methane and SH from a mixture **5** of adamantane and methane. A salient feature of this study is the development of methods that facilitate the growth of the single crystals. Since the method for all five systems is similar, only the process used for methane hydrate will be covered in detail. The method of refinement for the host lattice is described first followed by the guest molecules and the treatment of disorder.

Experimental Methods

A quartz capillary (0.3 mm diameter) was filled halfway with deionized water and then glued to an apparatus for handling gases at a vacuum line.⁸ With liquid nitrogen cooling, the relevant gases were then condensed onto the ice. The capillary was sealed using a hydrogen–oxygen torch, a procedure that has to be performed carefully to ensure that the end of the capillary is sealed tightly enough to maintain the pressure of the methane upon warming. The capillary was then transferred to the diffractometer, a SMART 1000 (Mo K α , graphite monochromator, $\lambda = 0.71073 \text{ \AA}$) equipped with a MSC X-STREAM low temperature device. A specially modified goniometer head with an additional arc was used to maintain the capillary parallel to the ω -axis to which the nozzle of the cold gas stream of the LT device was adjusted.

Below, approximately 7 °C a thin layer of solid gas hydrate is formed at the interface between the water and gas, producing a barrier that reduces the speed of crystal growth. The temperature varies somewhat with the pressure of methane in the capillary. Since gas hydrates melt incongruently with loss of gas, crystal growing procedures that are based on zone melting of the crystalline material could not be applied.

The best results were achieved when the mixture was heated repeatedly to the point of melting without allowing the gas to separate from the water, thereby increasing locally the gas content. This led to the formation of additional hydrate during the cooling cycle (about -2 °C). Single crystals were eventually obtained by allowing the polycrystalline material to anneal. This process took up to two weeks during which temperature parameters were controlled carefully.

These procedures lead to 'oligocrystalline' material which consisted of about 10 distinct gas hydrate single crystals of different sizes in arbitrary orientations depending on the position in the capillary and the progress of growth. These crystals were further surrounded by numerous smaller single crystals that are best described as polycrystalline material or powder.

Scintillation counter techniques do not allow data collection of oligocrystalline material. However, using an area detector and appropriate software it was possible to explore the complete reciprocal space by first harvesting all data and assessing them later. After thresholding the area detector frames and before applying the indexing procedure for each single crystal of the oligocrystalline material, an

additional step is required. It consists of separating all collected reflections into groups originating from each of the bigger single crystals. We used the program RLATT V3.0 and identified groups of reflections belonging to reciprocal lattices manually by visual inspection when rotating the spots and marking them. This time consuming task will probably be facilitated in the soon future.⁹

The procedure of measurement, separation, and indexing was repeated often during crystal growth, sometimes at different positions of the capillary, thus evaluating the progress of crystallization until a satisfactory state had been reached for a final measurement.

To avoid shifting of the oligocrystalline material during measurement at crystal growth temperature, the residual water is best transformed into a single ice crystal by repeated careful cooling and melting of the ice. Generation of a single crystal of ice is also helpful for a data acquisition at low temperature because there is a lower possibility of overlapping reflections.

1. The oligocrystalline material contained a twinned ice crystal and two crystals of gas hydrate of which only the strongest diffracting was used for subsequent processing. **2.** The oligocrystalline material contained an ice crystal and eight crystals of gas hydrate of which three of highest quality were used for subsequent processing. **3.** The oligocrystalline material contained an ice crystal and five crystals of gas hydrate of which only the strongest diffracting two were used for subsequent processing. **4.** Instead of water a 1:1 mixture of deionized water and ethanol was used. At the position of measurement only one crystal of gas hydrate filled the capillary. **5.** The oligocrystalline material contained an ice crystal and four crystals of gas hydrate of which only the strongest diffracting was used for subsequent processing.

A possible overlap of reflections from different crystals originating of the oligocrystalline material did not require special treatment. Even with crystals of almost the same orientation, the integration software SAINT V6.02a was able to separate the reflections. For such small lattice parameters, the reciprocal space is spacious enough to accommodate the reciprocal lattices of several single crystals without interfering overlap of reflections.

Absorption correction was performed on each crystal before merging with SADABS V2.03. Structure solution with statistical methods (BRUKER-SHELXS) was followed by full-matrix least-squares refinement on F^2 (BRUKER-SHELXTL-V6.12). Table 1 gives summary information on the crystallographic data.

Results

Structure of the Host Lattices. Each water molecule acts as hydrogen bond acceptor and a donor resulting in a tetrahedral environment of hydrogen bonds around the oxygen atoms as established within hexagonal ice. This leads to the rather loose packing of ice in the hexagonal tridymite lattice with unoccupied cavities of 1.5 to 2.8 Å diameter, low density, and other properties that make the water/ice system 'so nice to live in'.¹⁰

These features facilitate the formation of cages in the presence of small guest molecules resulting in encapsulation of the guest with no specific interactions other than van der Waals contacts, the energy gain is mostly based on entropy.¹⁰ Thus, structure of the hydrates depends on the size of the guest molecules so that the regular cages will only accommodate molecules up to a maximum size. All cages consist of nearly planar, hydrogen bonded four-, five-, and six-membered rings with O...O distances between $D = 2.725 \text{ \AA}$ and $D = 2.791 \text{ \AA}$. The cages are linked within the host framework by sharing common faces. Within experimental error, the structure of the host lattices is in accordance with the reported values.^{4,7,11}

(7) Gutt, C.; Asmussen, B.; Press, W.; Johnson, M. R.; Handa, Y. P.; Tse, J. S. *J. Chem. Phys.* **2000**, *113*, 4713–4721.

(8) Boese, R.; Nussbaumer, M. In *Organic Crystal Chemistry*; Garbarczyk, J. B., Jones, D. W., Eds.; Oxford University Press: Oxford, 1994; pp 20–37; www.ohcd-system.com.

(9) BrukerAXS, *RLATT Reciprocal Lattice Viewer Version 3*, **2000**; Wilson, C. C. *Acta Crystallogr.* **2001**, *B57*, 435–439.

(10) Kitaigorodsky, A. I. *Mixed Crystals*; Springer: Berlin, 1984; Vol. 33.

Table 1. Crystallographic Data Collection and Refinement Information

guest(s)	methane	acetylene	propane	propane, ethanol, methan	adamantane, methane
source	Merck 99.995%	Messer Griesheim 99.5%	Aldrich 98%	ethanol: Roth, 99.8%	Aldrich 99+%
empirical formula	(CH ₄) ₈ (H ₂ O) ₄₆	(C ₂ H ₂) _{7.2} (H ₂ O) ₄₆	(C ₃ H ₈) ₈ (H ₂ O) ₁₃₆	(C ₃ H ₈) ₈ (CH ₄) _{14.9} (H ₂ O) ₁₃₆	C ₁₀ H ₁₆ (CH ₄) ₅ (H ₂ O) ₃₄
measurement	740 frames with 0.3° scan width in ω , $\phi=0$, $\chi=0$, $d=5.121$ cm	780 frames with 0.3° scan width in ω , $\phi=0$, $\chi=0$, $d=4.457$ cm	740 frames each with $\theta = -32^\circ$ and $\theta = -42^\circ$, 0.3° scan width in ω , $\phi=0$, $\chi=0$, $d=4.457$ cm	780 frames with 0.3° scan width in ω , $\phi=0$, $\chi=0$, $d=4.410$ cm	760 frames with 0.3° scan width in ω , $\phi=0$, $\chi=0$, $d=4.457$ cm
<i>T</i>	123(2) K	143(2) K	123(2) K	163(2) K	123(2) K
crystal class	cubic	cubic	cubic	cubic	hexagonal
space group	<i>Pm</i> $\bar{3}$ <i>n</i>	<i>Pm</i> $\bar{3}$ <i>n</i>	<i>Fd</i> $\bar{3}$ <i>m</i>	<i>Fd</i> $\bar{3}$ <i>m</i>	<i>P6/mmm</i>
<i>a</i>	11.877(3) Å	11.895(3) Å	17.175(3) Å	17.1925(10) Å	12.3304(17) Å
<i>c</i>					9.9206(16) Å
volume	1675.6(8) Å ³	1683.0(8) Å ³	5066.0(15) Å ³	5081.8(5) Å ³	1306.2(3) Å ³
<i>Z</i>	1	1	1	1	1
μ	0.099 mm ⁻¹	0.104 mm ⁻¹	0.097 mm ⁻¹	0.101 mm ⁻¹	0.103 mm ⁻¹
<i>D</i> _{calc}	0.948 g cm ⁻³	1.023 g cm ⁻³	0.919 g cm ⁻³	1.000 g cm ⁻³	1.054 g cm ⁻³
no. of reflections:					
measured/crystal	6249	7096, 7118, 7090	5095, 4799	5489	5463
independent/crystal	475	480, 482, 475	372, 372	372	585
merged		482 (<i>R</i> _{merge} = 0.1093)	372 (<i>R</i> _{merge} = 0.0699)		
refinement	399 (<i>R</i> _{int} = 0.0743)	406	343	343 (<i>R</i> _{int} = 0.0240)	585 (<i>R</i> _{int} = 0.0545)
observed <i>F</i> _o > 2σ(<i>F</i>)	268	248	278	308	430
θ_{\max}	28.23°	28.25°	28.27°	28.24°	28.26°
parameters	30	41	37	40	65
restraints	0	3	0	2	
<i>R</i> 1 (<i>F</i>)	0.0379	0.0388	0.0465	0.0362	0.0438
<i>wR</i> 2 (all data)	0.0887	0.1418	0.0985	0.0931	0.1121
GoF(<i>F</i> ²)	1.094	1.269	1.159	1.074	1.110
max. res.e. dens.	0.214 eÅ ⁻³	0.214 eÅ ⁻³	0.342 eÅ ⁻³	0.257 eÅ ⁻³	0.246 eÅ ⁻³

Structure I is formed when water is co-condensed with methane to give **1** or with acetylene to give **2**. Both adopt the space group *Pm* $\bar{3}$ *n* *a* = 11.877(3) Å at 123(2) K. The dodecahedra cages are formed by the oxygen atoms which adopt a nearly body-centered arrangement with the central dodecahedron turned by 90°. Surrounding tetrakaidecahedra form columns along their hexagonal faces arranged vertically, horizontally and out of plane. See Figure 2.

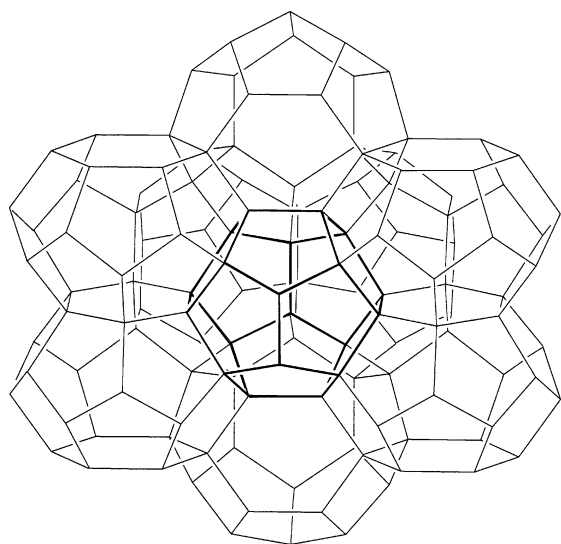


Figure 2. Packing of structure I gas hydrate. The outlined dodecahedron at the center is surrounded by eight tetrakaidecahedra.

Structure II is formed from propane resulting in **3** and also when crystals are grown from a mixture of propane and methane from water and ethanol to result in **4**. Addition of methane as a *help gas* facilitates crystal growth rates as does the addition of ethanol as a mediator. SII has space group *Fd* $\bar{3}$ *n* with *a* = 17.175(3) Å at 123(2) K. The hexakaidecahedra have tetrahedral symmetry and are linked with their four hexagonal faces in a

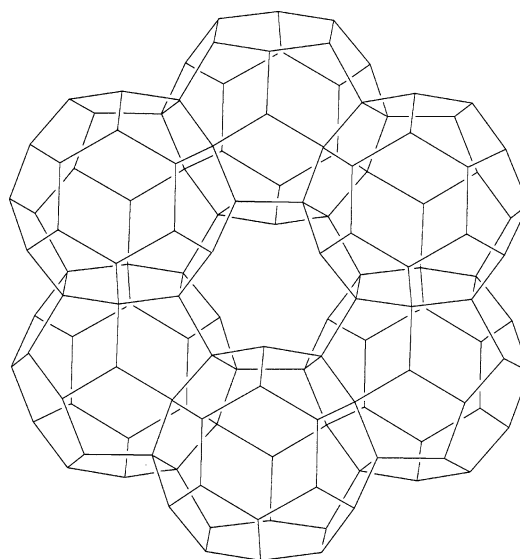


Figure 3. Packing of structure II gas hydrate. The hexakaidecahedra of tetrahedral symmetry form a diamondal network of which a six-membered ring is shown. The dodecahedra fill the voids within this network.

diamond-like structure. See Figure 3. A water molecule in the center of the remaining space occupies the common corner of four dodecahedra that fill this space.

Structure H (**5**) is formed when using a mixture of adamantane and methane as *help-gas*. It has the space group *P6/mmm* with *a* = 12.330 4(17) Å and *c* = 9.9206 (16) Å at 123(2) K. A central icosahedron is surrounded at its equator by six irregular dodecahedra which separate it from the neighboring, hexagonal-arranged icosahedra forming a layer. Two of these layers are connected on the top and bottom of the icosahedra while the remaining space is filled with regular dodecahedra. See Figure 4.

Filling of Cages with Guest Molecules. The refinement of guest molecules inside the cages is hampered by four additive

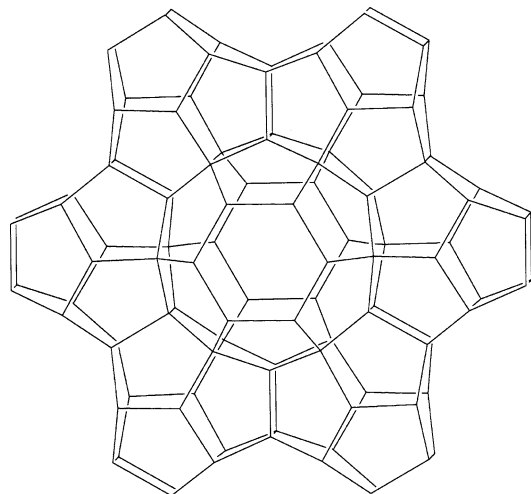


Figure 4. Packing of structure H gas hydrate. A central icosahedron is surrounded by six irregular dodecahedra.

types of disorder. First, the cages need not be filled stoichiometrically, lowering the over-all site occupation factor. Second, in the mixed hydrates **4** and **5**, the cages can be filled by different molecules creating a substitutional disorder. Third, the guest molecule can fit into the cage in different but distinct orientations thereby adopting the symmetry of the guest molecule to the higher symmetry of the cage. Fourth, the guest molecule can be too small to fill the cage and may not be centered. The symmetry of the host requires different centers of gravity of the guest that might result in dynamic positional disorder. It has been demonstrated by NMR spectroscopy that dynamical disorder occurs down to temperatures of a few Kelvin.¹²

Modeling of these types of disorder is difficult even when high-quality low-temperature neutron diffraction data of single crystals are available. With the experimental data at hand, the use of symmetry adapted functions for the scattering contribution of guest molecules does not seem to be particularly beneficial since the information that is gained is minimal.¹³ Therefore, electron density maps of the interior of the cages were carefully analyzed to obtain carbon and hydrogen atom positions adequate to model the electron density. Parameters were refined step by step. Great care was taken to obtain positional parameters, site occupation factors, and anisotropic displacement factors that are of physical significance, especially when these values have a tendency to be highly correlated. In some cases, distance restraints had to be applied and hydrogen atoms could not be included due to a low data-to-parameter ratio.

Methane in the Dodecahedral Cage. Methane has a molecular diameter of 4.3 Å, whereas the free diameter of the cage is 4.4 Å. This results in free rotation of the hydrocarbon. The electron density map shows a carbon atom at the center of the cage. This was found in all gas hydrate structures that contain methane in the dodecahedral cage.

In the methane hydrate **1**, the hydrogen atoms could be localized at $d_{\text{CH}} = 1.18(5)$ Å, disordered over twelve positions pointing at the center of the pentagons. In the mixed hydrate **4**,

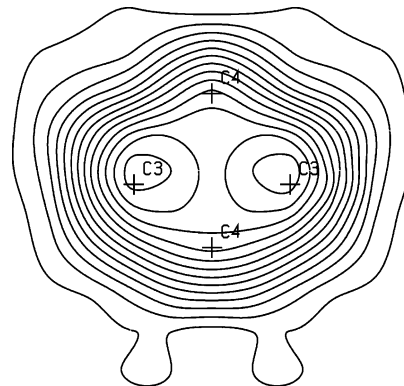


Figure 5. Electron density map of the tetrakaidecahedral cage in **2** perpendicular to the plane of the hexagons. Lines represent $0.2 \text{ e}\text{\AA}^{-3}$. In this view, the torus that is formed by rotation of acetylene results in two maxima named C3. The additional convexity at C4 corresponds to some of the acetylene molecules being out of plane.

the site occupation factor of the carbon atom refined to 0.93(2). Hydrogen atoms could be localized at 14 positions following the symmetry of the cage and were refined with a riding model. In the structure H (hydrate **5**), the site occupation factor in the regular dodecahedron is 0.92(2). In this case, an idealized model for the hydrogen atom positions was used leading to an overall site occupation factor of 0.7(1) for each of the four hydrogen atoms. In the irregular dodecahedron, the carbon atom site occupation factor is 0.872(17) and hydrogen atoms were incorporated with a riding model on idealized geometry.

Methane in the Tetrakaidecahedral Cage. The tetrakaidecahedral cage in **1** has a free diameter between 4.9 and 6.0 Å, giving even more space for methane than the dodecahedral cage in **1**. The electron density map suggests full disorder around the center of cavity. Accordingly, a single carbon atom was placed inside with the increased ADPs following the ellipsoidal shape of the cavity thus representing the dynamic disorder of the molecule. Eight hydrogen atom positions were generated in idealized geometry and refined with a riding model.

Acetylene in the Dodecahedral Cage. The length of acetylene (5.5 Å) prevents free rotation within the dodecahedral cage of **2**. The electron density is less spherically shaped than with methane and has a pronounced plateau at the center of the cage as would be expected for the molecular symmetry.

Following the symmetry of the cage, 18 carbon atom positions were taken from a Fourier map and restrained to keep the same distance from the center of the cage. The interatomic distance is $d_{\text{CC}} = 1.24(4)$ Å and the occupation factor refined to 0.6(1). The low occupation factor corresponds to the fact that molecules that are too large to fit easily within the cage will have lower stoichiometry.¹⁴

Acetylene in the Tetrakaidecahedral Cage. Although the dodecahedral cage in structure I is too small for acetylene, the long axis in the tetrakaidecahedral cage can accommodate the molecule. A section through the electron density depicts (in the drawing) two maxima belonging to a torus that winds along the equatorial plane of the cavity cage as illustrated in Figure 5. Residual electron density above and below this plane orients the acetylene molecule so that it points to the hexagonal faces. A similar electron density distribution was found with ethylene oxide.³

(11) Pauling, L.; Marsch, R. E. *Proc. Natl. Acad. Sci., U.S.A.* **1952**, *38*.
 (12) Ripmeester, J. A.; Ratcliffe, C. A.; Klug, D. D.; Tse, J. S. In *First International Conference on Natural Gas Hydrates*; Sloan, E. D., Happel, J., Hnatow, M. A., Eds., 1994; Vol. 715, p 161; Gutt, C.; Press, W.; Huller, A.; Tse, J. S.; Casalta, H. *J. Chem. Phys.* **2001**, *114*, 4160–4170.
 (13) Jagodzinski, H.; Frey, F. In *Reciprocal space*; Shmueli, U., Ed.; IUCr, Kluwer: Dordrecht, 2001; Vol. B.

(14) Sloan, E. D. *Clathrate Hydrates of Natural Gases*; Dekker: New York, 1998; p 55.

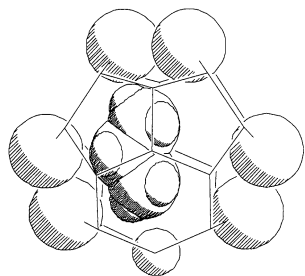


Figure 6. Size of the hexakaidecahedral cage in **3** is large enough to accommodate a propane molecule. All atoms are shown with their van der Waals radii. The small circle at the bottom symbolizes the position of a O–H···O hydrogen bond.

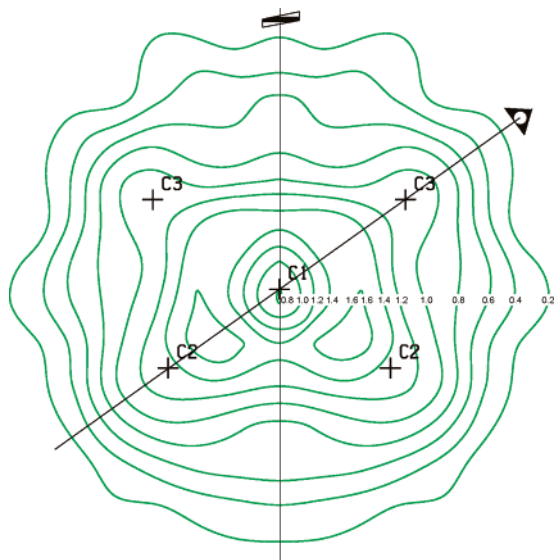


Figure 7. Electron density map of the hexakaidecahedral cage in **3** in the plane of both symmetry axes. Lines represent $0.2 \text{ e}\text{\AA}^{-3}$ and refined positions of atoms are indicated. The electron distribution is almost spherical with a local minimum at the center.

Following the symmetry of the cage, four carbon atom positions in the torus and two perpendicular to it, were taken from the Fourier map for refinement. The distance across the torus was restrained to $1.15(1) \text{ \AA}$, modeling a carbon–carbon triple bond. The sum of occupancies is $1.1(1)$ indicating that the cage is fully occupied.

Propane in the Hexakaidecahedral Cage. The hexakaidecahedral cage in propane hydrate **3** has a free diameter of 6.8 \AA , while the propane molecule measures a maximum of 6.3 \AA . Therefore, free rotation is inevitable. Figure 6 shows the available space in the cavity in relation to the guest molecule. The electron density map supports this conclusion. A distribution close to spherical symmetry with a local minimum at the center of the cage is depicted in Figure 7. This was taken as proof that the center of the cage is not occupied and the propane molecules are situated at the wall of the cage. A similar electron density distribution was found for tetrahydrofuran hydrate,³ which has rather different spacial requirements.

Following symmetry of the cage, 14 carbon atom positions were taken from the Fourier map for free refinement. If the center of the cage was considered to be empty, the refinement was not stable until a fourth atom was introduced into this position. The sum of occupancy factors is $1.3(7)$ molecules of propane, which indicates that the site is fully occupied. The

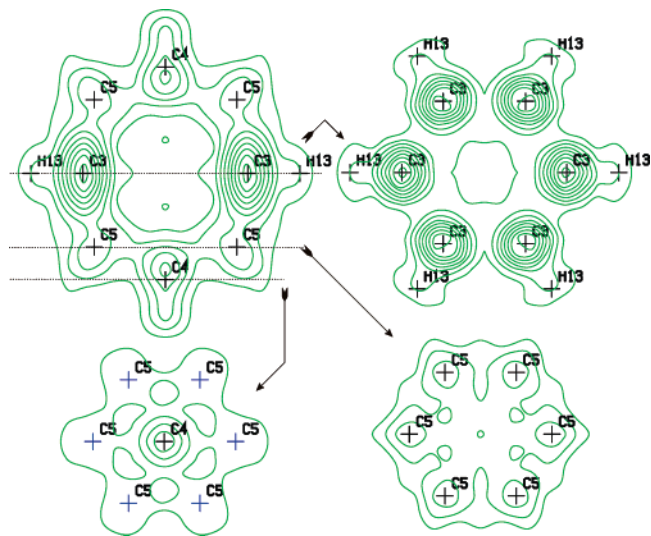


Figure 8. Electron density maps of the icosahedral cage in **5**. Lines represent $0.5 \text{ e}\text{\AA}^{-3}$. The top-left depicts the $(\bar{1} 2 1)$ -plane, the others are perpendicular to the 6-fold axis as indicated. Refined atom positions are included. In contrast to the other cages separated maxima are found.

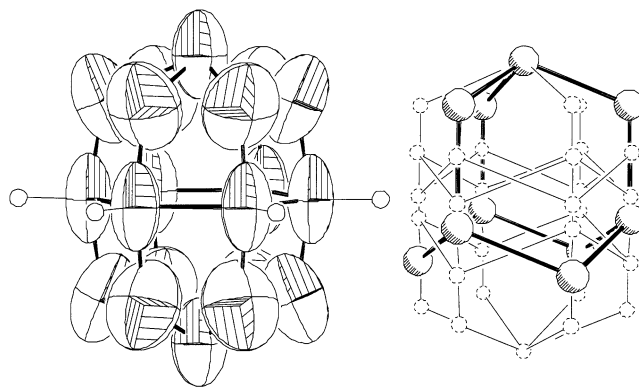


Figure 9. Contents of the icosahedral cage in **5**. left: refined atom position and ADPs. right: model of 4-fold disorder of an adamantane molecule, which explains the experimentally found electron density distribution. Hydrogen atoms are not included.

high standard deviation is due to intrinsic difficulties in modeling the disorder and to high correlation of the refined parameters.

In the pure propane hydrate **3**, the dodecahedral cage is empty as expected. The residual electron density is $0.14 \text{ e}\text{\AA}^{-3}$.

In the mixed hydrate **4**, the situation inside the hexakaidecahedral cage is analogous to the pure propane hydrate **3** resulting in the same type of modeling with one exception. In this case, the maximum of electron density resides at the center of the cage. The maximum electron density could be due to substitutional disorder from methane, but this is less likely since the overall occupation factor corresponds to $1.7(3)$ molecules of propane, which could not be achieved by methane alone. Occupation of two molecules per cage at the applied pressure is also highly unlikely.^{1,15}

Adamantane in the Icosahedral Cage. The equatorial free diameter of the icosahedral cage is 7.2 \AA , but it reduces vertically so that 2.5 \AA above the equatorial plane, halfway to the polar hexagon, the free diameter is only 5.8 \AA . This does not provide enough space for rotation of the adamantane

(15) Mao, W. L.; Mao, Ho-k.; Goncharov, A. F.; Struzhkin, V. V.; Guo, Q.; Hu, J.; Shu, J.; Hemley, R. J.; Somayazulu, M.; Zhao, Y. *Science* **2002**, *297*, 2247–2249.

molecule where the corresponding values are 7.1 and 6.5 Å. In accordance with this, the electron density map has separated maxima. See Figure 8.

Following $6/mmm$ symmetry, twenty carbon atom positions were taken from the Fourier map and refined freely. The sum of carbon atom occupancies is 9(1), which matches full occupancy of the cage with $C_{10}H_{16}$. Only six hydrogen atoms in the equatorial plane could be found from a Fourier map. They are pointing toward the centers of the hexagonal faces.

Figure 9 depicts a comparison of the modeled electron density by the carbon atom positions and accompanying anisotropic displacement parameters. This type of electron density distribution can be explained in terms of a 4-fold, static disorder of the adamantane molecule as shown at the right side of the model.

Conclusion

We have described an experimental method to cocrystallize gases and liquids (or solutions) by filling the components into a capillary with in situ crystallization as the cocrystallization is followed by X-ray diffraction measurements. The process results in an 'oligocrystal' rather than a single crystal. Data treatment therefore includes the separation of superimposed reciprocal lattices. Data collected simultaneously can be merged, thereby enhancing coverage and data quality. We propose to call the technique oligo diffractometry.¹⁶

By cocrystallization of water with organic compounds, hydrates of methane, acetylene, propane, a propane/ethanol/methane-mixture, and an adamantane/methane-mixture were obtained. Cell parameters are in accord with reported values.⁵ Host networks and guests are subject to extensive disorder, which reduces the reliability of structural information. As expected, the features of the host network are not influenced by the chemical nature of the guest as only size determines the type of host structure that is formed.

(16) Boese, R.; Kirchner, M. T.; Billups, E.; Norman, L. R. *Angew. Chem., Int. Ed. Engl.* **2003**, *42*, 1961–1963.

The disorder in the cages is attributed to the absence of directionality of intermolecular interactions. Thus methane in the dodecahedral and propane and methane in the tetrakaidecahedral cages can be considered as free rotors. Acetylene barely fits the dodecahedral cage and will only rotate free in the equatorial plane of the tetrakaidecahedral cage. A disordered model with four distinct orientations is proposed for adamantane in the icosahedral cage.

It was found that all cages are nearly fully or fully occupied within the limits of the estimated standard deviations. Of course there are intrinsic uncertainties in the refinement methods of the guest molecules with the exception of the dodecahedral cage in the acetylene hydrate which is filled to about 60%. The absolute values of the occupation, however, should always be viewed with the esds and accordingly treated with care. In all cases, it is not clear to what extent the cages must be filled to prevent collapse of the lattice.

With oligo diffractometry we have shown that it is possible to gain insight into the structural requirements of multicomponent liquid solutions, especially for cocrystals of liquids with gases.¹⁷ We plan to carry out additional studies on solutions of gases in organic solvents in order to provide a deeper understanding of multicomponent systems.

Acknowledgment. R.B. and M.T.K. thank the Deutsche Forschungsgemeinschaft SFB 452 for financial support. W.E.B. is supported by the National Science Foundation and the Welch Foundation.

Supporting Information Available: X-ray crystallographic data for structure determinations (CIF). This material is available free of charge via the Internet at <http://pubs.acs.org>.

JA049247C

(17) On the basis of neutron diffraction experiments, which show that methane molecules in solution are physically dissolved and surrounded by small clathrate-like cages, the structure in the solid may be thought of as a frozen liquid situation: Koh, C. A.; Wisbey, R. P.; Wu, X. P.; Westacott, R. E.; Soper, A. K. *J. Chem. Phys.* **2000**, *113*, 6390–6397.